Journal of Materials Chemistry C

RSC Publishing

PAPER

View Article Online
View Journal | View Issue

Cite this: J. Mater. Chem. C, 2013, 1, 6145

A silver nanocube on a gold microplate as a well-defined and highly active substrate for SERS detection

Xiaohu Xia,[a] Matthew Rycenga,[b] Dong Qin[c] and Younan Xia*[ad]

Received 16th April 2013
Accepted 22nd May 2013

DOI: 10.1039/c3tc30707g

www.rsc.org/MaterialsC

Strong enhancement and good reproducibility in Raman signals are two major requirements for a surface-enhanced Raman scattering (SERS) substrate to be used for sensitive detection of an analyte. Here we report a new type of SERS substrate that was fabricated by depositing a Ag nanocube (AgNC) on the surface of a Au microplate (AuMP). Owing to the strong and reproducible hot spots formed at the corner sites of the AgNC in proximity to the AuMP surface, the new substrate showed high sensitivity and reproducibility. Using 1,4-benzenedithiol as a probe, the SERS enhancement factor of a typical "AgNC on AuMP" substrate could reach a level as high as 4.7×10^7. In addition to the high sensitivity and reproducibility, the "AgNC on AuMP" substrate also displayed very good stability. The potential use of the "AgNC on AuMP" substrate was demonstrated by detecting crystal violet with high sensitivity.

Introduction

Surface-enhanced Raman scattering (SERS) is a fascinating phenomenon in which the Raman scattering cross-sections of molecules are dramatically enhanced when they are adsorbed on certain metal substrates (Au and Ag nanoparticles in most cases, due to their surface plasmon resonance peaks in the visible region[1]).[2–4] Owing to its ability to greatly amplify the Raman signals from an analyte, SERS has emerged as an attractive technique for applications involving sensitive detection.[5–7] In general, large enhancement of Raman signals often occurs at particular sites, the so-called hot spots, rather than over the entire substrate.[8–10] Hot spots can be defined as gaps or junctions between two or more closely spaced particles where enhancement of local electric fields often arises, in contrast to individual particles.[11,12] In general, hot spots are desired for high-sensitive detection. The commonly used method for preparing SERS substrates with hot spots relies on the uncontrolled aggregation of Ag or Au nanoparticles that is induced by a salt or self-assembly process.[13,14] While these nanoparticle aggregates can provide strong enhancement factors (EFs) up to 10^{14}, the poor reproducibility associated with the fabrication process as well as the shape irregularity of the hot-spot regions impose many challenges for the reproducible preparation of SERS substrates.[15]

In contrast to the strategy of nanoparticle aggregation, we have recently reported a novel approach to the generation of hot spots with sufficiently strong SERS EFs up to 10^8 by simply depositing Ag nanocubes (AgNCs) on the surface of an Ag or Au thin film.[16] The hot spots were created at the corner sites of the AgNC that are in proximal contact with its supporting metal film. This approach is better controlled in comparison with methods based on nanoparticle aggregation since hot spots form automatically during the cast deposition of AgNCs. Moreover, this new approach produces SERS substrates with highly accessible hot spots for sensitive detection since the hot spots are located outside the junction between the nanocubes and the metal support. Despite these demonstrations, there is still one drawback for this new SERS substrate that is caused by the relatively rough surface of the metal film prepared by thermal evaporation (typically with a root-mean-square surface roughness of 5 nm).[16] This rough surface may cause irregularity for the hot spots at the corner sites of an AgNC and thereby poor reproducibility for the SERS substrate. In the present study, we replaced the thermally evaporated metal film with ultra flat Au microplates (AuMPs, with a root-mean-square surface roughness of 0.4 nm) to generate a new type of SERS substrate, called the "AgNC on AuMP" substrate, which should have well-defined hot spots and thus improved reproducibility. In addition to the good reproducibility, the "AgNC on AuMP" substrate was also shown with high SERS enhancement and considerable stability. The potential use of the "AgNC on AuMP" substrate was demonstrated by detecting crystal violet with high sensitivity and good reproducibility.

[a]The Wallace H. Coulter Department of Biomedical Engineering, Georgia Institute of Technology and Emory University, Atlanta, Georgia 30332, USA. E-mail: younan.xia@bme.gatech.edu

[b]Department of Chemistry, Northwestern University, Evanston, Illinois 60208, USA

[c]School of Materials Science and Engineering, Georgia Institute of Technology, Atlanta, Georgia 30332, USA

[d]School of Chemistry and Biochemistry and School of Chemical and Biomolecular Engineering, Georgia Institute of Technology, Atlanta, Georgia 30332, USA

Experimental

Syntheses of AgNCs and AuMPs

The AgNCs with an average edge length of 100 nm were prepared using seed-mediated growth according to our previously reported procedures.[17] Briefly, 20 mL of ethylene glycol (EG) was added into a 100 mL flask and heated in an oil bath to 150 °C under magnetic stirring. Then, 6.0 mL of EG containing 120 mg poly(vinyl pyrrolidone) (PVP, $M_w \approx 55\,000$) was added using a pipette. After 10 min, 200 μL of the suspension of 40 nm Ag cubic seeds in EG ($\sim 5.0 \times 10^{12}$ particles per mL) was introduced, followed by the addition of 4.0 mL of $AgNO_3$ solution (282 mM, in EG) using a pipette. The 40 nm cubic seeds were prepared using a recently reported protocol.[18] The 100 nm AgNCs were obtained by quenching the reaction with an ice-water bath when the major local surface plasmon resonance (LSPR) peak of the product had reached ~585 nm. The product was washed with acetone once and deionized (DI) water twice prior to re-dispersion in 1.0 mL of DI water for further use. The AuMPs were prepared using a previously reported protocol with minor modifications.[19] In a typical synthesis, 1.0 mL of $HAuCl_4$ (0.2 M) aqueous solution was added to 6.0 mL of EG held at 150 °C under gentle stirring. Then, 3.0 mL of EG containing 600 mg PVP was added dropwise using a pipette. The AuMPs were obtained by quenching the reaction with an ice-water bath when the reaction had been progressed for 45 min. The product was rinsed with acetone once and DI water five times prior to storing in 2.0 mL of DI water.

Fabrication of the "AgNC on AuMP" substrate

The "AgNC on AuMP" substrate was prepared using a two-step procedure: (i) drop-casting 2 μL of the as-prepared AuMP suspension on a silicon (Si) wafer that had been patterned with registration marks and letting it dry under ambient conditions and (ii) deposition of AgNCs functionalized with probe molecules onto the AuMPs. In the latter case, we drop-cast 2 μL of AgNCs ($\sim 5 \times 10^{11}$ particles per mL) pre-functionalized with 1,4-benzenedithiol (1,4-BDT) (details for functionalization can be found in our previously published work[16]) onto the AuMPs deposited on a Si wafer and letting it dry under ambient conditions. During the process of solvent evaporation, the "AgNC on AuMP" substrates would form *via* random deposition of AgNCs onto the surfaces of AuMPs. The "AgNC on AuMP" substrates were then washed with copious amounts of ethanol, and finally dried under a stream of air. All the "AgNC on AuMP" substrates were used immediately for SERS measurements right after preparation.

Characterizations

The SERS spectra were recorded using a Renishaw inVia confocal Raman spectrometer coupled to a Leica microscope with a 50× objective (N.A. = 0.90). The light source at 785 nm was from a semiconductor cw diode laser and used with a holographic notch filter with a grating of 1200 lines per millimeter. The back-scattered Raman signals were collected on a thermoelectrically cooled (−60 °C) CCD detector. SERS data were collected with $\lambda_{ex} = 785$ nm, $P_{laser} \approx 0.6$ mW and $t = 20$ s. Processing of the SERS spectra and all data analyses were done with IGOR Pro software (Portland, OR). All data were baseline corrected before normalization. For baseline correction, a fourth order polynomial was fitted to the raw SERS spectrum and subtracted. Scanning electron microscopy (SEM) images were taken using an FEI field-emission microscope (Nova NanoSEM 230) operated at an accelerating voltage of 15 kV. Atomic force microscopy (AFM) data were collected in the tapping mode using a Nanoscope V Multimode SPM (Veeco Instruments, Santa Barbara, CA). The probes were 125 mm long, phosphorus-doped Si tips (with a nominal tip radius of 10 nm, MPP-11100-10, Veeco Probes). The images were collected with drive frequencies of 312–320 kHz and a scan rate of 1 Hz. Topography features were measured using the Nanoscope 7.20 software from the same company. Plasma etching was performed in a plasma cleaner/sterilizer (Harrick Scientific Corp., PDC-001) operated at 60 Hz and 0.2 Torr of air, with power being set to high. In a typical process, the sample was placed in a plasma cleaner chamber and exposed to the oxygen plasma for 6 min.

Results and discussion

Characterization of the "AgNC on AuMP" substrate

Fig. 1(a) shows the SEM image of the as-prepared AgNCs of 100 nm in average edge length, which had a uniform distribution in terms of both shape and size. It should be pointed out that all the six side faces of an AgNC possess atomically smooth surfaces as shown in our previous studies.[20,21] Fig. 1(b) shows the SEM image of the as-prepared AuMPs with an average lateral size of 20 μm. Most of these AuMPs had either a hexagonal or truncated triangular shape (see the insets). As indicated by the AFM data in Fig. 1(c), the AuMPs had ultra flat surfaces with a root-mean-square surface roughness of ~0.4 nm and an average thickness of 80 nm. The atomically flat surfaces for both AgNCs and AuMPs ensure the formation of well-defined hot spots at the corner sites of an AgNC in proximity to the AuMP surface.

The "AgNC on AuMP" substrate, fabricated by casting AgNCs onto AuMPs (see the Experimental section for details), can be conveniently located under a dark-field optical microscope during SERS measurements. The detailed morphologies of an "AgNC on AuMP" substrate can be revealed by SEM imaging after SERS measurements. Fig. 2(a) shows a dark-field optical micrograph of a region containing an "AgNC on AuMP" substrate (the blue dot labeled *1* together with the yellow hexagonal frame) and an individual AgNC that was located outside the AuMP (*i.e.*, directly on Si wafer, the blue dot labeled *2*). Fig. 2(b) shows the SEM image of the same region shown in Fig. 2(a), where the two AgNCs are circled and labeled in the SEM image to help identify them. Fig. 2(c) and (d) show SEM images of both AgNCs at a higher magnification, clearly demonstrating that the AgNCs had a cubic profile with sharp corners.

SERS properties of the "AgNC on AuMP" substrate

We firstly recorded SERS spectra from an individual 1,4-BDT-functionalized AgNC that was deposited on an AuMP with

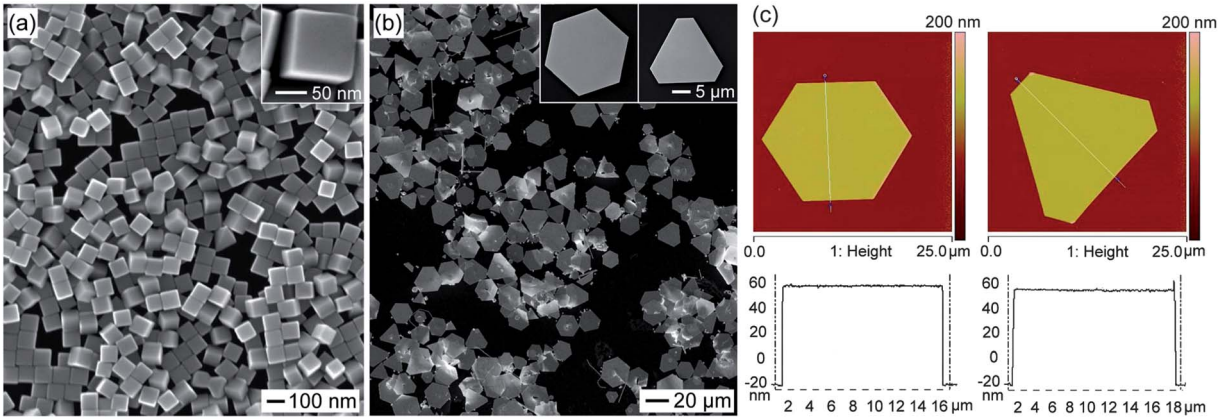

Fig. 1 (a) SEM image of the as-prepared 100 nm AgNCs. The inset shows the SEM image of an individual AgNC at a higher magnification. (b) SEM image of the as-prepared AuMPs. The insets show two typical types of AuMPs at higher magnifications, which had hexagonal (left) and truncated triangular (right) profiles, respectively. (c) AFM data recorded from two typical types of AuMPs. The thicknesses and root-mean-square surface roughness of both AuMPs were measured to be approximately 80 nm and 0.4 nm, respectively.

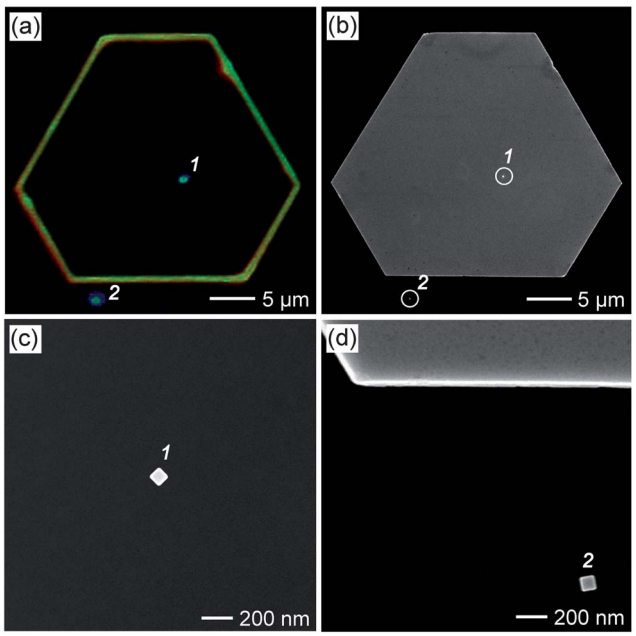

Fig. 2 (a) Dark-field optical micrograph of an "AgNC on AuMP" substrate that was deposited on a Si wafer. The AgNCs (small dots) labeled *1* was on top of an AuMP while the one labeled *2* was directly deposited on the Si wafer. (b) SEM image of the same region as shown in (a). (c and d) SEM images of AgNCs *1* and *2*, respectively, at a higher magnification.

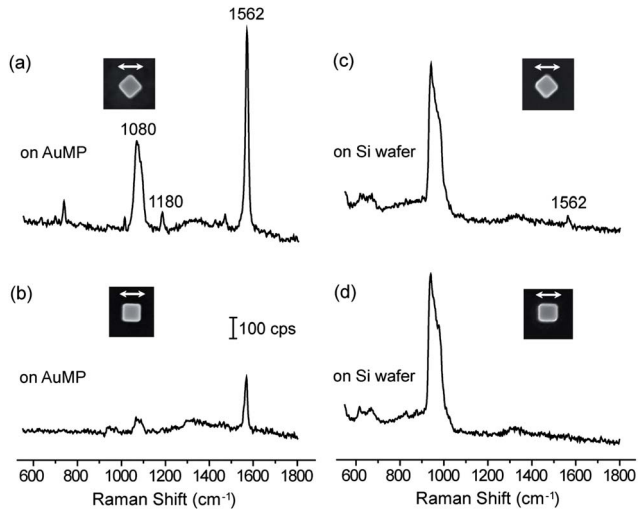

Fig. 3 Comparison of the SERS spectra recorded from two 1,4-BDT-functionalized AgNCs that were deposited on (a and b) an AuMP, and (c and d) Si wafer. Insets are the SEM images of the AgNCs. The double arrow on each SEM image denotes the polarization of incident laser. The scale bar in (b) applies to all the spectra in (a–d).

785 nm laser excitation. After SERS measurements, we used SEM to collect information about the size, shape, and orientation of the AgNC using a process known as SERS-SEM correlation.[22] Fig. 3(a) and (b) show SERS spectra taken from a single AgNC deposited on an AuMP at different azimuthal angles relative to the polarization of excitation laser with the help of a specially designed rotation stage.[21] The peaks at the positions of 1080, 1180, and 1562 cm^{-1} can be ascribed to the vibrations of 1,4-BDT, where the bands at 1562 and 1180 cm^{-1} are associated with modes ν_{8a} and ν_{9a} and the band at 1080 cm^{-1} can be indexed to the ν_1 fundamental in Fermi resonance with a combination mode consisting of $\nu_{6a} + \nu_{7a}$.[23,24] It can be observed that the 1,4-BDT signals were strongly dependent on laser polarization. When the AgNC was orientated with a diagonal axis (corner to corner) parallel to the laser polarization, see Fig. 3(a), the peak was about 3 times stronger than the case when the AgNC was oriented with one of the side faces parallel to the polarization of the laser, see Fig. 3(b).

In order to quantify the SERS enhancements of the "AgNC on AuMP" substrate, we employed the peaks at 1562 cm^{-1} (the strongest band in the 1,4-BDT spectra) to calculate the SERS EFs for the "AgNC on AuMP" substrate using the following equation:[23,25]

$$EF = (I_{SERS} \times N_{bulk})/(I_{bulk} \times N_{SERS})$$

where I_{SERS} and I_{bulk} are the intensities of the same band for the SERS and bulk spectra; N_{bulk} is the number of molecules probed for a bulk sample; and N_{SERS} is the number of molecules probed with SERS. N_{bulk} was determined based on the ordinary Raman spectrum of a 0.1 M 1,4-BDT solution in 12 M aqueous NaOH and the focal volume of our Raman system (1.48 pL). When determining N_{SERS}, we assumed that the 1,4-BDT molecules were adsorbed as a monolayer with molecular footprints of 0.19 nm^2,[22,23] and a surface area of 10 000 nm^2 was calculated for a single AgNC, according to their shape and size (Fig. 1(a)). Based on the spectra shown in Fig. 3(a) and (b), the EF for the "AgNC on AuMP" substrate was calculated to be 4.7×10^7 when the AgNC was orientated with a diagonal axis parallel to the laser polarization. In comparison, the EF dropped to 1.5×10^7 when the AgNC was orientated with one of the edges parallel to the laser polarization. It is worth pointing out that the EFs for the "AgNC on AuMP" substrate should be even higher when a shorter-wavelength laser (*e.g.*, 514 nm laser) rather than 785 nm laser is used for excitation because it matches better with the LSPR peak of the AgNCs.[26] In the present study, we chose a 785 nm laser as the excitation source because we are most interested in using the "AgNC on AuMP" substrate for the detection of biological species where the near-infrared laser is preferred to diminish the background fluorescence.[5,27]

For comparison studies, we also recorded SERS spectra from another individual 1,4-BDT-functionalized AgNC that was directly deposited on the Si wafer under the same experimental conditions, see Fig. 3(c) and (d). The broad band at 900–1000 cm^{-1} can be attributed to the Si substrate.[28] In this case, the intensities of the 1562 cm^{-1} band were found to be ~30 times lower than the case when the AgNC was deposited on an AuMP with the same laser polarizations. These results again demonstrated the formation of hot spots at the corner sites of an AgNC in proximity to the AuMP surface with exceptionally strong enhancements.

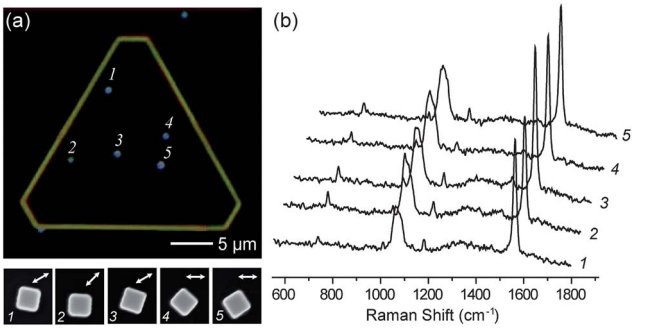

Fig. 4 (a) Dark-field optical micrograph of five different 1,4-BDT-functionalized AgNCs that were deposited on top of the same AuMP. The bottom panel shows SEM images of the corresponding AgNCs that are labeled with the same numbers as in the micrograph. (b) SERS spectra recorded from the five AgNCs shown in (a), with the polarizations of incident laser being aligned parallel to the face diagonal of each AgNC.

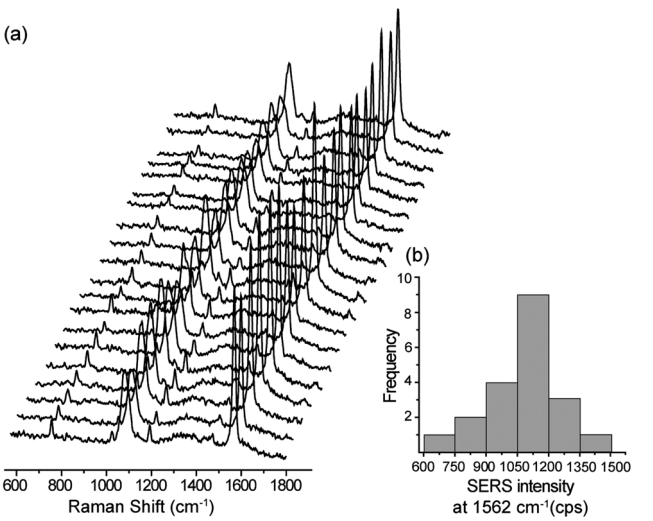

Fig. 5 (a) SERS spectra recorded from 20 individual 1,4-BDT-functionalized AgNCs that were deposited on 20 different AuMPs. The polarization of incident laser was aligned parallel to the face diagonal of each AgNC. (b) Histogram of the SERS intensity of the 1562 cm^{-1} bands based on the spectra shown in (a).

Reproducibility and stability

Since the SERS enhancement of the "AgNC on AuMP" substrate had a strong dependence on the direction of laser polarization as mentioned above, the direction of laser polarization needs to be fixed in order to test its reproducibility and stability. For this purpose, in the following discussion, all the SERS spectra were chosen and analyzed only when the AgNCs were orientated with one of their face diagonal axes parallel to the laser polarization. We first examined the reproducibility of the "AgNC on AuMP" substrate by conducting the following two sets of experiments. In the first set of experiments, we recorded SERS spectra from different AgNCs that were located on the same AuMP. Fig. 4 compares the SERS spectra recorded from five different 1,4-BDT-functionalized AgNCs deposited on the same AuMP. It is clear that all the spectra were consistent in terms of both intensity and peak position. In the second set of experiments, we recorded SERS spectra from 20 1,4-BDT-functionalized AuNCs that were deposited on 20 different AuMPs. As shown in Fig. 5, the spectra also display good consistence. These observations indicate that the "AgNC on AuMP" substrate has a considerable reproducibility, which can be attributed to the ultra flat surfaces of both AgNCs and AuMPs and thereby the well-defined hot spots. To test the stability of the "AgNC on AuMP" substrate, we recorded SERS spectra from a 1,4-BDT-functionalized AgNC deposited on an AuMP as a function of time. As shown in Fig. 6, the SERS spectra recorded at different time points with a period of 20 min only showed some minor variations in terms of both peak position, see Fig. 6(a), and intensity, see Fig. 6(b).

Detection of crystal violet

Finally, we demonstrated the potential use of the "AgNC on AuMP" substrate by detecting crystal violet (CV), a kind of unapproved drug that is effective against fungal and parasite infections in fish,[29] in stock solutions with different concentrations. The detection includes the following steps: (i)

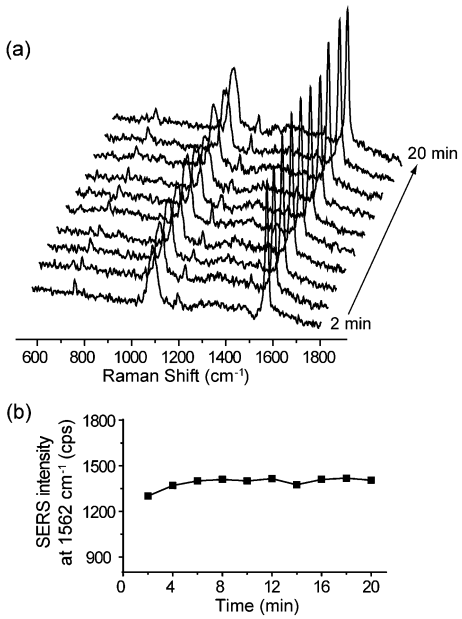

Fig. 6 (a) SERS spectra recorded from the same 1,4-BDT-functionalized AgNC that was deposited on an AuMP at 2 min intervals for 20 min. (b) Variation of the SERS intensity of the 1562 cm^{-1} band based on the spectra shown in (a) as a function of time, where the average SERS intensity and standard deviation are calculated to be 1405.2 and 51.9 cps, respectively.

incubating an ethanol suspension of AgNCs (1 nM in particle concentration) with CV stock solutions of known concentrations in ethanol for 2 h; (ii) drop-casting 2 μL of the suspension on AuMPs that were pre-deposited on a Si wafer; (iii) drying the substrate under ambient conditions, followed by brief rinse with ethanol and drying again; and (iv) recording SERS spectra from the CV-decorated AgNCs with their diagonal axis being aligned parallel to the laser polarization. Fig. 7(a) shows the representative spectra taken from three different AgNCs that were incubated with 500, 50 and 20 ppb of CV standard solutions, respectively. SERS spectra of the 500 ppb CV solution exhibited strong characteristic Raman peaks, the positions of which were in good agreement with the previously reported data,[30,31] indicating that the "AgNC on AuMP" substrate had a good specificity in detecting CV. The intensities of the main peak at 1619 cm^{-1} decreased monotonously with the decrease in CV concentration. The SERS peaks were still distinguishable when the CV concentration dropped to 20 ppb. The coefficients of variation ($n = 12$) across the whole range are below 30% as shown in Fig. 7(b). These results demonstrate that the "AgNC on AuMP" substrate could be used as a promising SERS imaging agent for high-sensitive detection with good specificity and reproducibility.

Conclusions

In summary, we have demonstrated a new SERS substrate that can be fabricated by depositing AgNCs onto the surface of AuMPs. The SERS enhancement factors of such "AgNC on AuMP" substrates could reach a level as high as 4.7×10^7. Owing to the well-defined hot spots formed at the corner sites of an AgNC in proximity to the AuMP surface, the "AgNC on AuMP" substrate also showed good reproducibility. The "AgNC on AuMP" substrate was further applied to the detection of crystal violet with good specificity and high sensitivity. It is expected that the "AgNC on AuMP" substrate demonstrated in this work will find applications in SERS detection for a wide range of analytes.

Acknowledgements

This work was supported in part by an NIH Director's Pioneer Award (DP1 OD000798), a grant from the NCI (R01 CA13852701), and start-up funds from Georgia Institute of Technology.

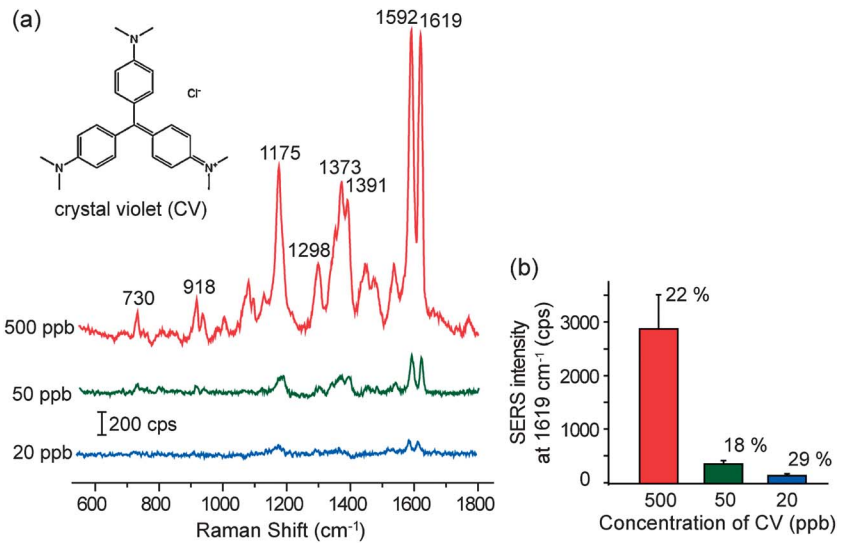

Fig. 7 (a) Representative SERS spectra of crystal violet (CV) standard solutions of different concentrations that were measured using the "AgNC on AuMP" substrate. (b) Concentration variation of the SERS intensity of the 1619 cm^{-1} band. The error bars indicate the standard deviation from 12 independent measurements.

References

1 M. Kerker, *J. Opt. Soc. Am. B*, 1985, **2**, 1327.
2 K. A. Willets and R. P. Van Duyne, *Annu. Rev. Phys. Chem.*, 2007, **58**, 267.
3 R. K. Chang and T. E. Furtak, *Surface Enhanced Raman Scattering*, Plenum Press, New York, 1982.
4 A. Aroca, *Surface-Enhanced Vibrational Spectroscopy*, John Wiley & Sons, New York, 2006.
5 X. M. Qian, X. H. Peng, D. O. Ansari, Q. Yin-Goen, G. Z. Chen, D. M. Shin, L. Yang, A. N. Young, M. D. Wang and S. M. Nie, *Nat. Biotechnol.*, 2008, **26**, 83.
6 X. Zhang, M. A. Young, O. Lyandres and R. P. Van Duyne, *J. Am. Chem. Soc.*, 2005, **127**, 4484.
7 D. S. Grubisha, R. J. Lipert, H.-Y. Park, J. Driskell and M. D. Porter, *Anal. Chem.*, 2003, **75**, 5936.
8 A. Otto, *J. Raman Spectrosc.*, 2006, **37**, 937.
9 W. E. Doering and S. Nie, *J. Phys. Chem. B*, 2002, **106**, 311.
10 E. C. Le Ru, P. G. Etchegoin and M. Meyer, *J. Chem. Phys.*, 2006, **125**, 204701.
11 Z. Wang, S. Pan, T. D. Kraus, H. Du and L. J. Rotheberg, *Proc. Natl. Acad. Sci. U. S. A.*, 2003, **100**, 8638.
12 E. C. Le Ru, M. Meyer, E. Blackie and P. G. Etchegoin, *J. Raman Spectrosc.*, 2008, **39**, 1127.
13 K. Kneipp, H. Kneipp, I. Itzkan, R. R. Dasari and M. S. Feld, *Chem. Rev.*, 1999, **99**, 2957.
14 R. G. Freeman, K. C. Grabar, K. J. Allison, R. M. Bright, J. A. Davis, A. P. Guthrie, M. B. Hommer, M. A. Jackson, P. C. Smith, D. G. Walter and M. J. Natan, *Science*, 1995, **267**, 1629.
15 S. Nie and S. R. Emory, *Science*, 1997, **275**, 1102.
16 M. Rycenga, X. Xia, C. H. Moran, F. Zhou, D. Qin, Z.-Y. Li and Y. Xia, *Angew. Chem., Int. Ed.*, 2011, **50**, 5473.
17 X. Xia, J. Zeng, L. K. Oetjen, Q. Li and Y. Xia, *J. Am. Chem. Soc.*, 2012, **134**, 1793.
18 Q. Zhang, W. Li, L. P. Wen, J. Chen and Y. Xia, *Chem.–Eur. J.*, 2010, **16**, 10234.
19 C. Kan, X. Zhu and G. Wang, *J. Phys. Chem. B*, 2006, **110**, 4651.
20 Y. Sun and Y. Xia, *Science*, 2002, **298**, 2176.
21 J. M. McLellan, Z.-Y. Li, A. R. Siekkinen and Y. Xia, *Nano Lett.*, 2007, **7**, 1013.
22 M. Rycenga, P. H. C. Camargo, W. Li, C. H. Moran and Y. Xia, *J. Phys. Chem. Lett.*, 2010, **1**, 696.
23 S. W. Joo, S. W. Han and K. Kim, *J. Colloid Interface Sci.*, 2001, **240**, 391.
24 S. H. Cho, H. S. Han, D. J. Jang, K. Kim and M. S. Kim, *J. Phys. Chem.*, 1995, **99**, 10594.
25 P. H. C. Carmargo, C. M. Cobley, M. Rycenga and Y. Xia, *Nanotechnology*, 2009, **20**, 434020.
26 A. D. McFarland, M. A. Young, J. A. Dieringer and R. P. Van Duyne, *J. Phys. Chem. B*, 2005, **109**, 11279.
27 R. S. Golightly, W. E. Doering and M. J. Natan, *ACS Nano*, 2009, **3**, 2859.
28 P. H. C. Camargo, M. Rycenga, L. Au and Y. Xia, *Angew. Chem., Int. Ed.*, 2009, **48**, 2180.
29 E. J. Liang, X. L. Ye and W. Kiefer, *J. Phys. Chem. A*, 1997, **101**, 7330.
30 T. Watanabe, *Chem. Phys. Lett.*, 1982, **6**, 501.
31 M. V. cañamares, C. Chenal, R. L. Birke and J. R. Lombardi, *J. Phys. Chem. C*, 2008, **112**, 20295.